Preprint
UCRL-JC-141574-Rev-1

Visualization of Mixing and Combustion in TNT Explosions

A. L. Kuhl, R. E. Ferguson, A. K. Oppenheim, M. R. Seizew

This article was submitted to
Extreme States of Substance Detonation Shock Waves, Sarov, Nizhni Novgorod Region, Russia, February 26-March 3, 2001

March 26, 2001

U.S. Department of Energy

Lawrence Livermore National Laboratory

This work was performed under the auspices of the United States Department of Energy by the University of California, Lawrence Livermore National Laboratory under contract No. W-7405-Eng-48.

UCRL-JC-141574 Rev. I

Visualization of Mixing and Combustion in TNT Explosions

A. L. Kuhl, R. E. Ferguson[1], A. K. Oppenheim[2] & M. R. Seizew[3]
Lawrence Livermore National Laboratory, Livermore, CA

Abstract

Numerical simulations are used to visualize the mixing and combustion induced by explosions of spherical and cylindrical TNT charges. Evolution of the exothermic energy is controlled by mixing (vorticity), which is strongly influenced by wave reflections from confining walls.

Approach

Described here are numerical simulations of combustion in explosions created by the detonation of solid TNT charges in air. The problem was formulated as turbulent combustion in unmixed gases (Zel'dovich, 1949), where the expanded TNT detonation products play the role of a fuel. We consider the limit of large Reynolds, Peclet and Damköhler numbers— where molecular transport processes are negligible. This perspective results in a gasdynamic Model of combustion in explosions (Kuhl et al, 1997 & 1999). The Model equations were integrated numerically by a higher-order Godunov scheme (Colella & Glaz, 1985). A block-structured, Adaptive Mesh Refinement algorithm (Bell et al, 1994) was used to resolve the energy-bearing scales of turbulent mixing on the computational grid. The effects of mixing and combustion were visualized by displays of material fields (*yellow*=Fuel, *blue*=Air & *red*= Products), vorticity and dilatation contours, and exothermic fields (*white* stars) as shown in the accompanying figures.

Visualization

The detonation wave in the TNT charge transforms the solid explosive ($C_7H_5N_3O_6$) to gaseous products that are rich in carbon solid and carbon monoxide. The 210-kbar detonation pressure causes the products to expand rapidly, driving a blast wave into the surrounding air (Brode, 1959). The interface between the products and air is unstable (Meshkov, 1960), and rapidly evolves into a turbulent mixing layer (Anisimov & Zel'dovich, 1977; Kuhl, 1996) illustrated in Fig. 1. The blast wave contains an embedded shock (inside the TNT interface), which draws the Taylor cavities into the origin as it implodes. Thus air becomes distributed throughout the hot detonation products gases causing rapid combustion as shown in Fig. 2.

Figure 3 presents the details of the flow field for the corresponding confined-explosion case at an earlier scaled time ($t = 0.01 ms/g^{1/3}$). There one can observe the main shock, its initial reflection from the chamber walls, and its interaction with embedded shock. Combustion occurs in the fine-scale mixing structures on the TNT interface. For *spherical charges*, vorticity concentrates in *rings* (Fig. 4), which causes the mixing structures to acquire a mushroom-shaped form (Fig. 3). As time progresses, the vortex rings interact, forming successively more and more complex mixing structures.

Figure 5 illustrates the flow field from a cylindrical TNT charge in a cylindrical enclosure at somewhat later times ($t = 0.2$ & $0.5 ms/g^{1/3}$). The corresponding blowup views (Fig. 6)

[1]Krispin Technologies, Rockville, MD [2] University of California, Berkeley, CA [3] Logicon, Los Angeles, CA

show details of the flow field near a large combustion structure. In the limit of large Peclet and Damköhler numbers considered here, combustion is concentrated in thin exothermic sheets. Expansion of combustion products along a sheet induces vorticity layers on either side of the sheet—forming, in effect, an *exothermic doublet* that continues to supply fuel and oxidizer to the combustion process through local entrainment.

Figure 7 shows an 3-D view of the corresponding vorticity field. For *cylindrical charges*, vorticity concentrates into *filaments* that interact forming *hairpin structures* where the vorticity becomes unbounded. This signals the transition to fully developed turbulent flow (Bell & Marcus, 1992) via the baroclinic mechanism.

Figure 8 depicts the pressure history on the chamber wall from the 3-D AMR simulation compared with the experimental measurement; agreement is excellent, especially for comparisons of point measurements in 3-D turbulent fields. The corresponding case of a nitrogen atmosphere (i.e., explosion only) illustrates the dramatic effect that combustion creates in such confined explosions.

To systematically explore the effect of confinement, simulations were performed in four geometrically similar chambers (right circular cylinders with $H = D$, **1:** $D_1 = 12cm$ & $V_1 = 1.4l$, **2:** $D_2 = 20cm$ & $V_2 = 6.3l$, **3:** $D_3 = 40cm$ & $V_3 = 50l$, **4:** $D_4 = 80cm$ & $V_4 = 402l$). Figures 9 and 10 visualize the evolution of combustion in the four cases, where rows correspond to cases and columns represent fixed times. They show that shock reflections from chamber walls stir up the mixing layer, thereby changing the burning rate.

The chamber pressure histories for the four cases are plotted in Fig. 11. It shows that combustion increases the late-time overpressure by 3.5 times (if there is enough oxygen available to oxidize all the fuel, i.e., Cases 2-4). The corresponding fuel consumption curves are presented in Fig. 12, illustrating that the burning rate depends on chamber side.

Résumé

These numerical simulations illustrate a combustion regime that is controlled by turbulent mixing, in contrast to the conventional reaction-diffusion mechanism first proposed by Zel'dovich & Frank-Kamenetskii (1938).

References

Anisimov, S. I., and Zel'dovich, Ya. B. (1977) "Rayleigh-Taylor Instability of Boundary between Detonation Products and Gas in Spherical Explosion", *Pis'ma Zh. Eksp. Teor. Fiz.*, **3**, 1977, pp. 1081-1084.

Bell, J. B., and Marcus, D. L. (1992) "Vorticity Intensification and Transition to Turbulence in the 3-D Euler Equations", *Comm. Math. Phys.*, **147**, 1992, pp. 374-394.

Bell, J. B., Berger, M., Saltzman, J., Welcome, M. (1994) "Three-Dimensional Adaptive Mesh Refinement for Hyperbolic Conservation Laws," *SIAM J. Scientific & Statistical Computing*, **15** (1), 1994, pp. 127-138.

Brode, H. L. (1959) "Blast Wave from a Spherical Charge, *Physics of Fluids* **2** (2), pp 217-229 (also "*A Calculation of a Blast Wave from a Spherical Charge of TNT"*, **RM-1965**, Rand, Santa Monica, CA, 1947).

Colella, P. and Glaz, H. M. (1985) "Efficient Solution Algorithms for the Riemann Problem for Real Gases", *J. Computational Physics*, **59** (2), 1985, pp. 264-289.

Meshkov, E. E. (1960) "Instability of the Interface of Two Gases Accelerated by a Shock Wave", *Izv AN SSRE Mekhanika Zhidkosti i Gaza*, **4** (15), 1960, pp. 151-157.

Kuhl, A. L. (1996) "Spherical Mixing Layers in Explosions", *Dynamics of Exothermicity*, J. R. Bowen Ed., Gordon and Breach, Longhorn, PA (1996), pp. 291-320.

Kuhl, A. L., Ferguson, R. E., and Oppenheim, A. K. (1997) "Gasdynamic Model of Turbulent Exothermic Fields in Explosions", *Advances in Combustion Science—in Honor of Ya. B. Zel'dovich*, A. Merzhanov, L. DeLuca & W. Sirignano Eds., *Prog. Astro. & Aero.*, **173**, AIAA, Washington, DC (1997), pp. 251-261.

Kuhl, A.L., Ferguson, R.E., and Oppenheim, A.K. (1999) "Gasdynamics of Combustion of TNT Products in Air", *Archivum Combustionis*, **19**(1-4), 1999, pp. 67-89.

Zel'dovich, Ya. B., and Frank-Kamenetzkii, D. A. (1938) "A Theory of Thermal Propagation of Flame", *ACTA Physico-Chimica URSS*, **9** (2), 1938, pp. 341-350.

Zel'dovich, Ya. B. (1949) "K Teorii Goreniya Ne Peremeshannykh Gazov" ("On the Theory of Combustion of Initially Unmixed Gases") *Zh. Tekh. Fiz.*, **19**(10), 1949, pp. 1199-1210.

Acknowledgements

This work was performed under the auspices of the U. S. Department of Energy by the University of California, Lawrence Livermore National Laboratory under Contract No. W-7405-Eng-48.

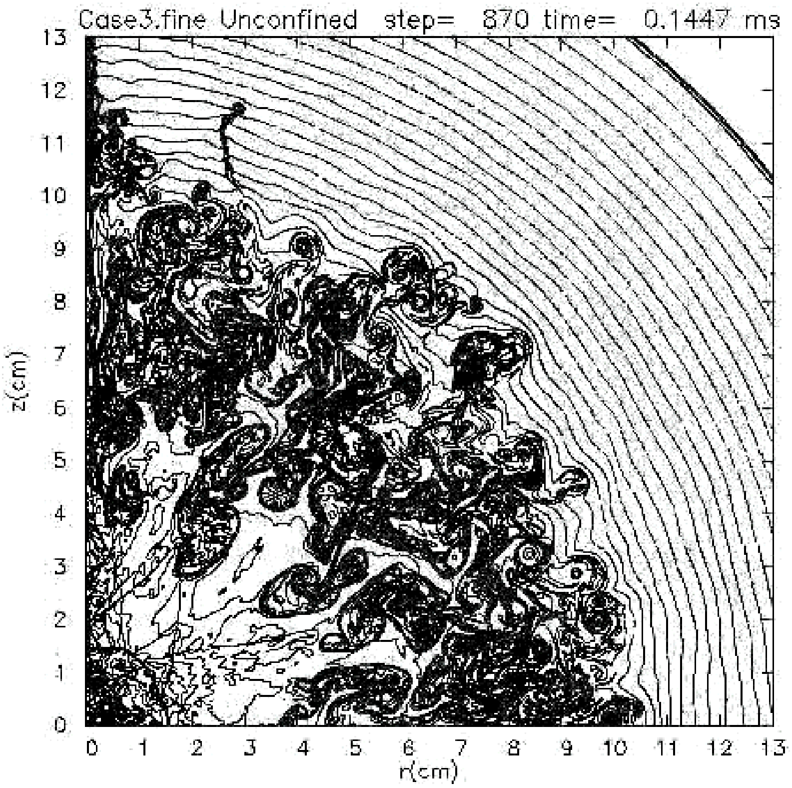

Figure 1. Mixing in an unconfined explosion of a 1-g TNT sphere in air (density contours at $t = 0.144 ms$).

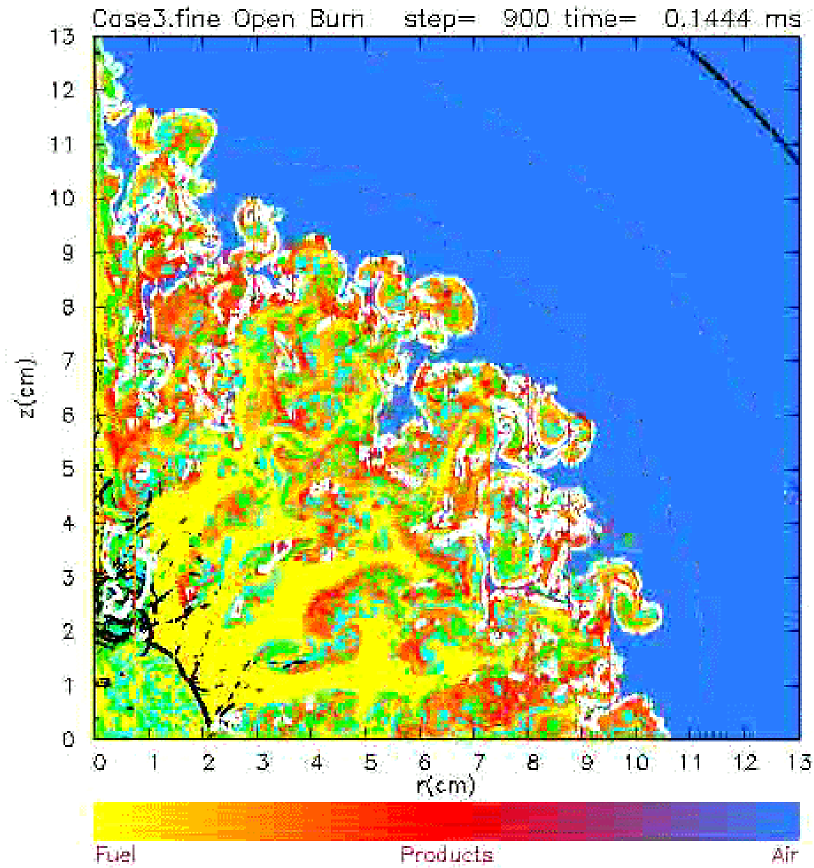

Figure 2. Combustion in an unconfined explosion of a 1-g TNT sphere in air ($t = 0.144\,ms$).

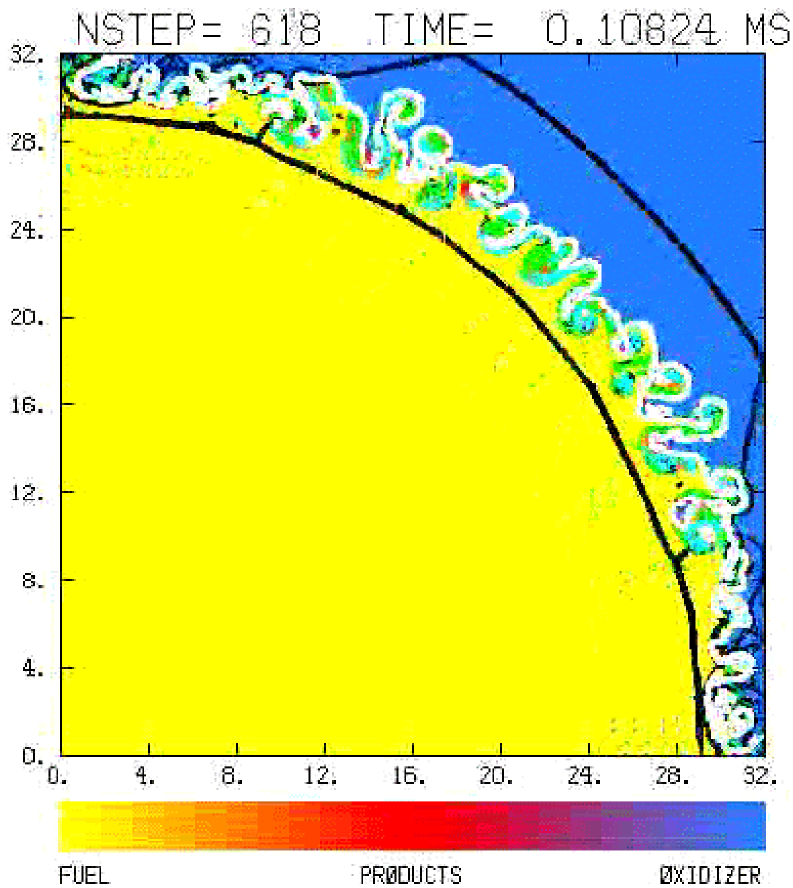

Figure 3. Combustion of the detonation products from a 1-kg TNT sphere in a cylindrical calorimeter filled with air ($t = 0.01 ms / g^{1/3}$).

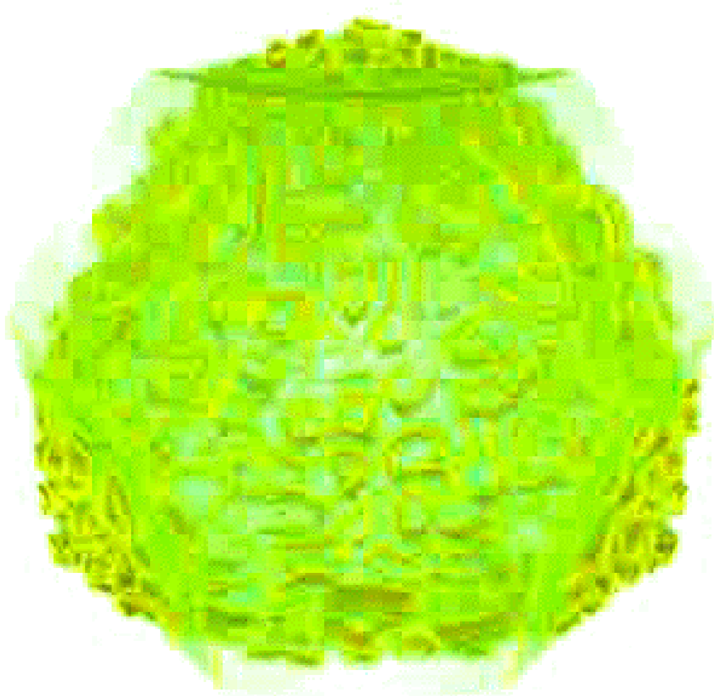

Figure 4. Vorticity concentration into vortex rings on the HE-air interface formed during combustion of a 1-kg TNT sphere in a cubical calorimeter.

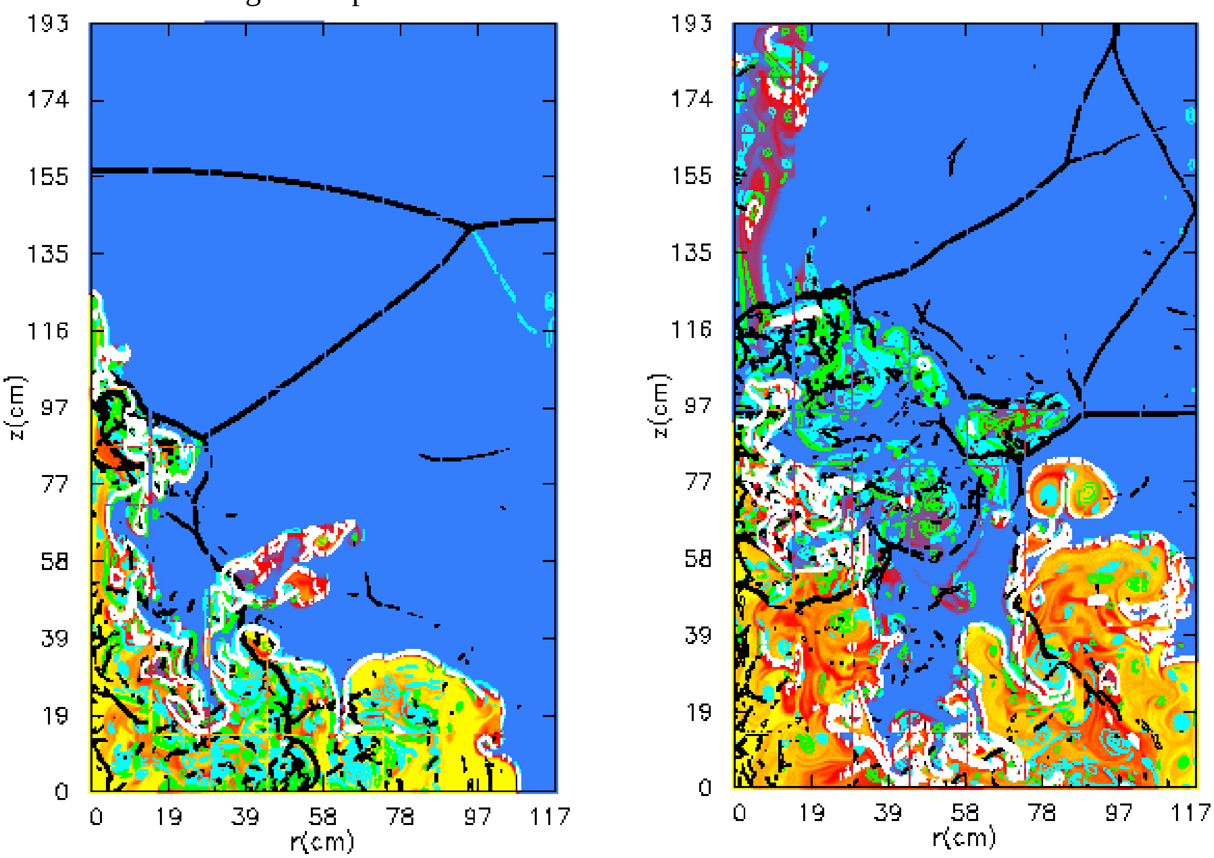

Figure 5. Combustion of detonation products from a 0.9-kg TNT cylinder in a $16.6\,m^3$ cylindrical tank; overall view of the flow field at $t = 0.2$ & $0.5\,ms/g^{1\,/}$.

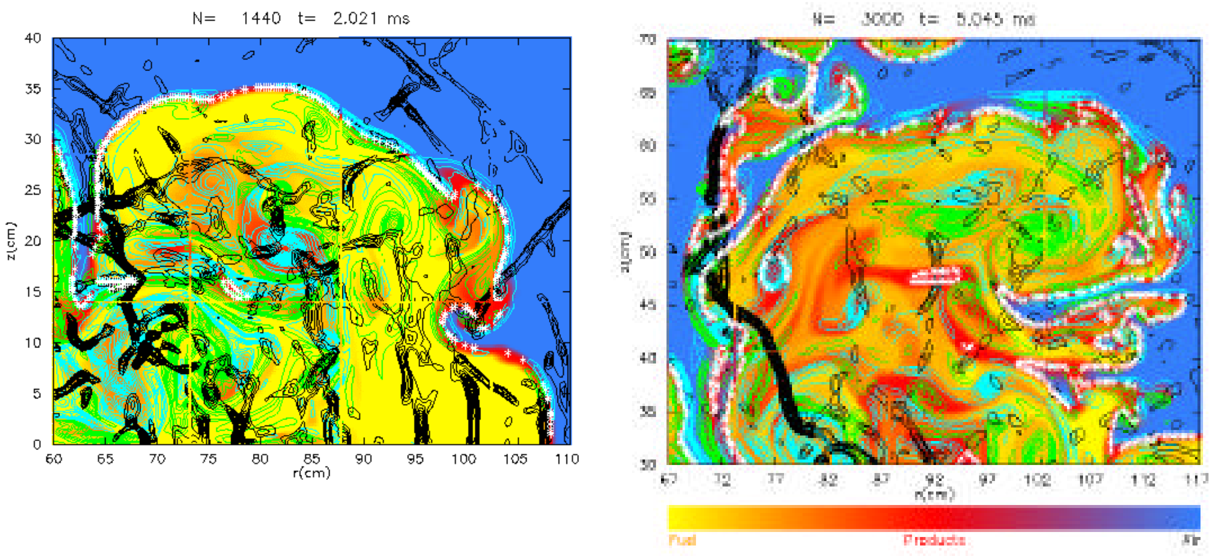

Figure 6. Blow-up views of the flow field near a large combustion structure.

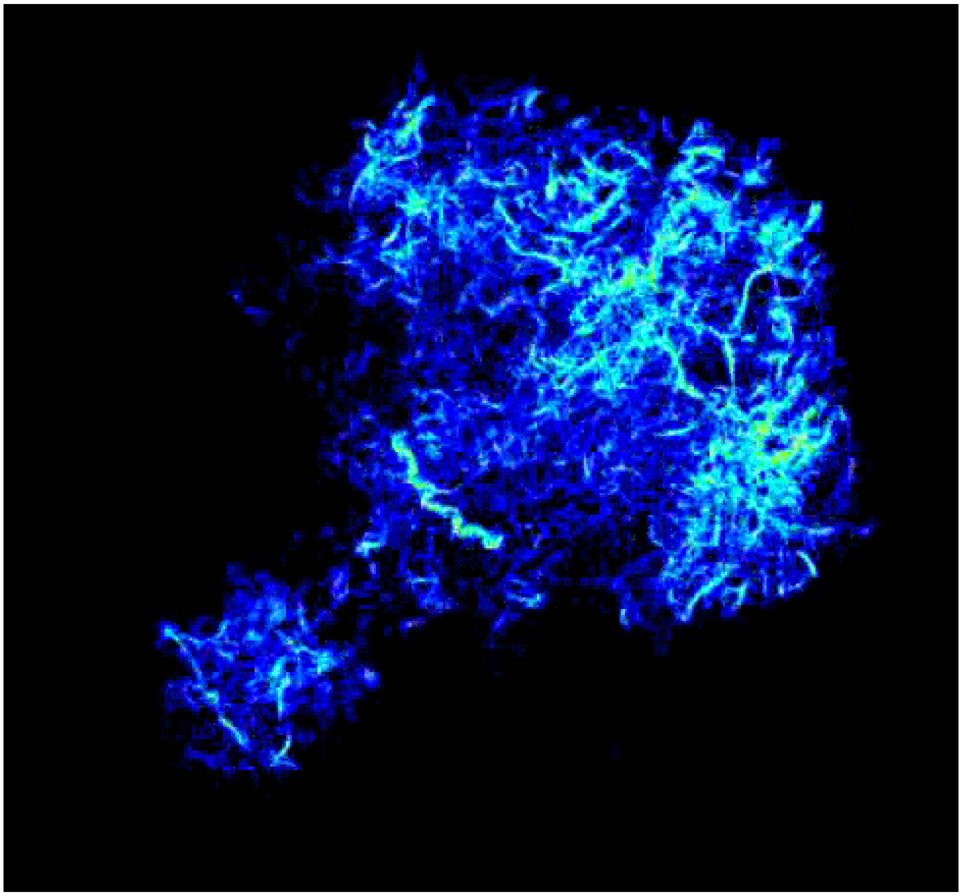

Figure 7. Vorticity filamentation during the combustion of a 1-kg TNT cylinder (see Fig. 5).

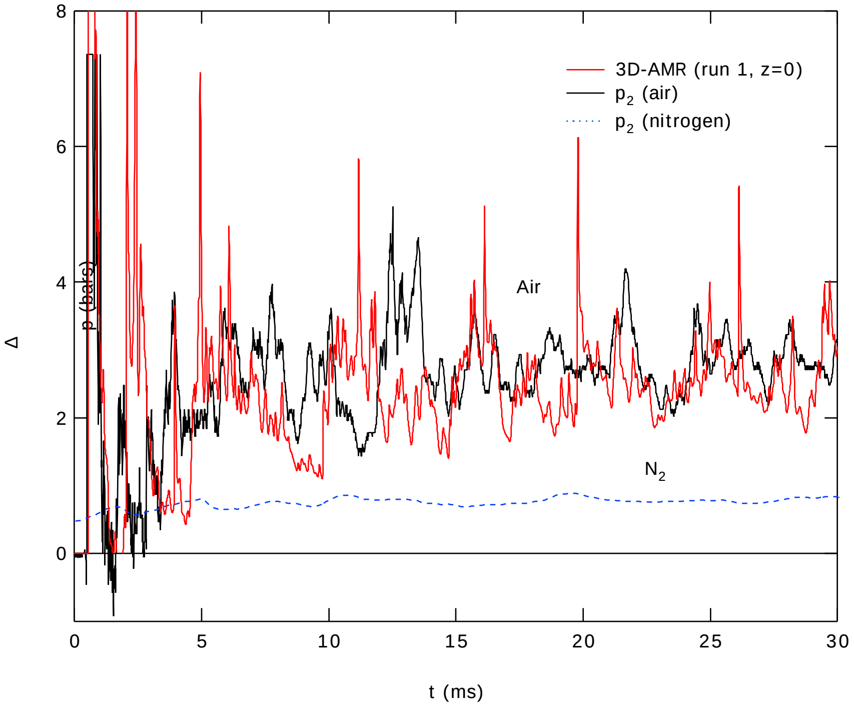

Figure 8. Comparison of calculated static pressure history on the wall with data for combustion of a 0.9-kg TNT cylinder shown in Figures 5-7.

Case 1: t = 0.02 ms

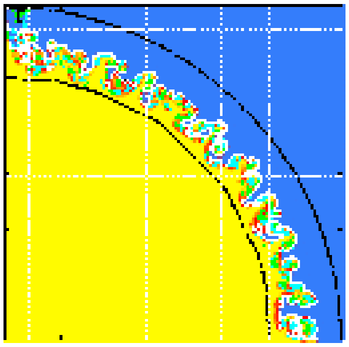

Case 1: t = 0.05 ms

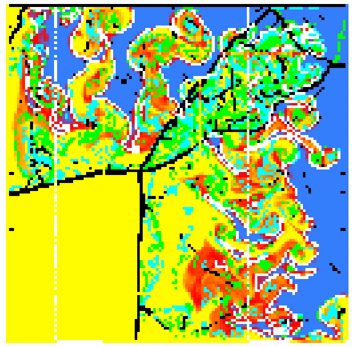

Case 1: t = 0.20 ms

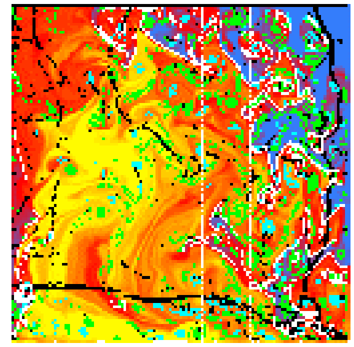

Case 2: t = 0.02 ms

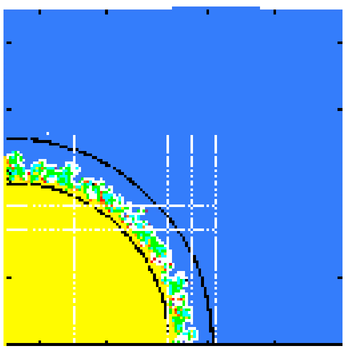

Case 2: t = 0.05 ms

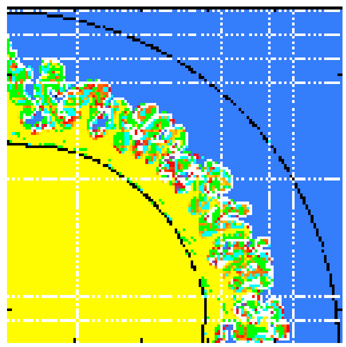

Case 2: t = 0.20 ms

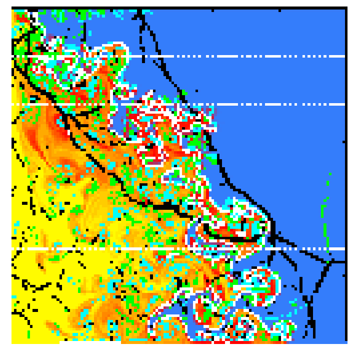

Case 3: t = 0.02 ms

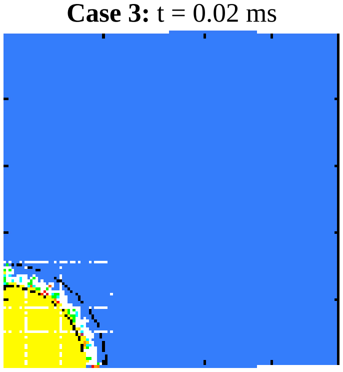

Case 3: t = 0.05 ms

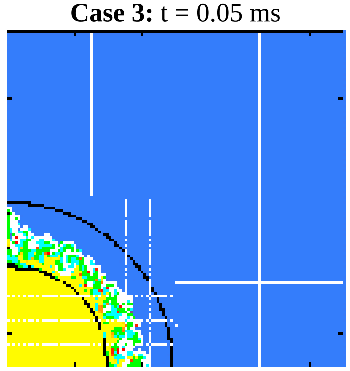

Case 3: t = 0.20 ms

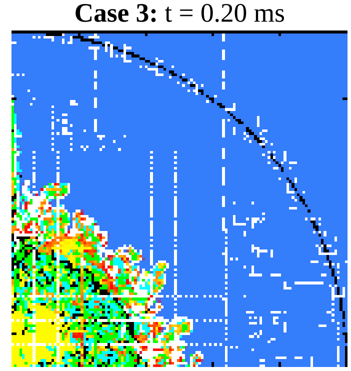

Case 4: t = 0.02 ms

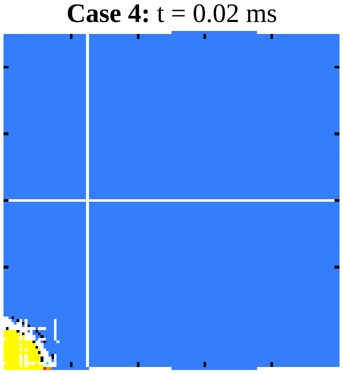

Case 4: t = 0.05 ms

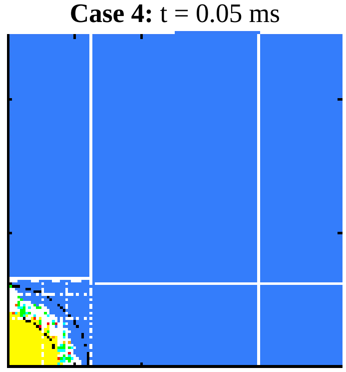

Case 4: t = 0.20 ms

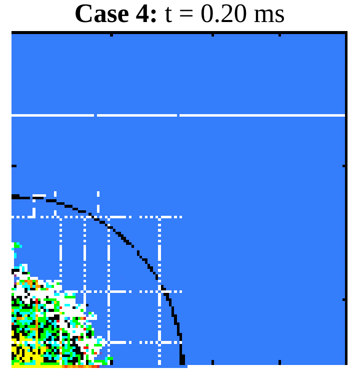

Figure 9. Early-time evolution of combustion of detonation products from a 1-g TNT sphere with air in different chambers (**1**: $D_1 = 12cm$, **2**: $D_2 = 20cm$, **3:** $D_3 = 40cm$, **4**: $D_4 = 80cm$).

Case 1: t = 0.60 ms

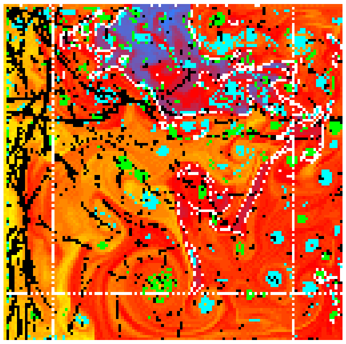

Case 1: t = 1 ms

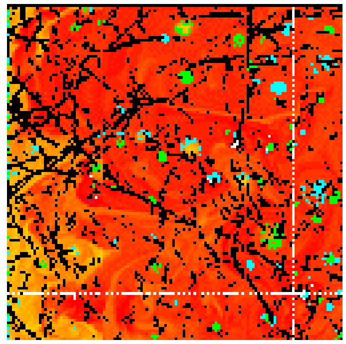

Case 1: t = 1.6 ms

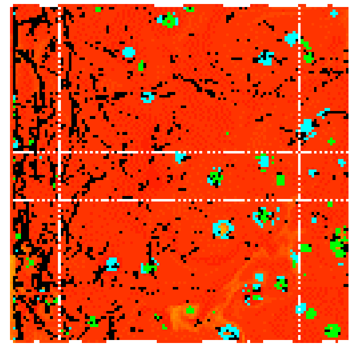

Case 2: t = 0.60 ms

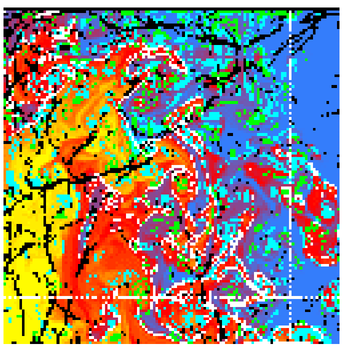

Case 2: t = 1 ms

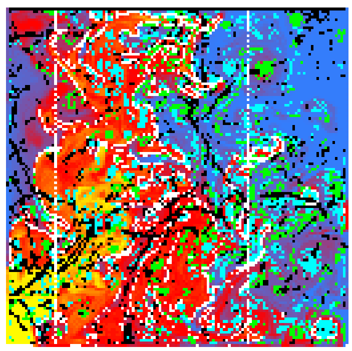

Case 2: t = 3.6 ms

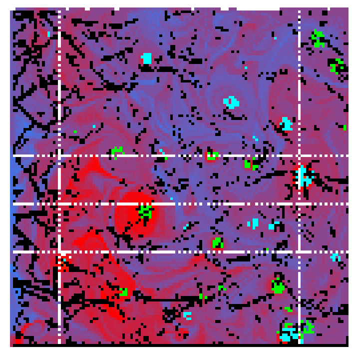

Case 3: t = 0.60 ms

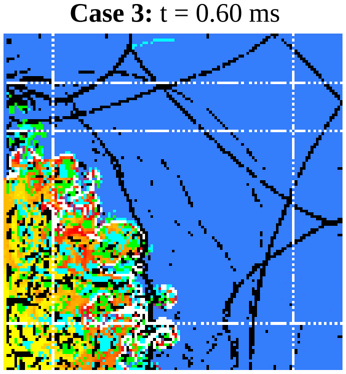

Case 3: t = 1 ms

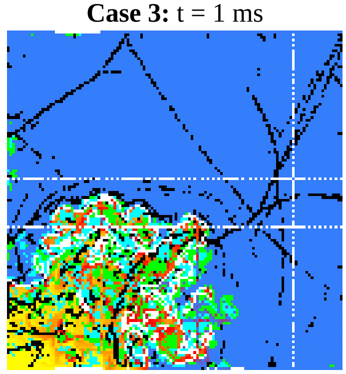

Case 3: t = 4 ms

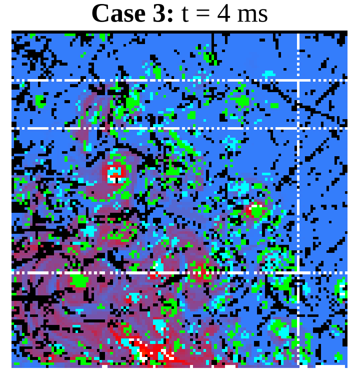

Case 4: t = 0.60 ms

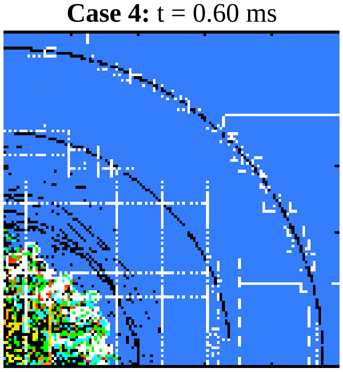

Case 4: t = 1 ms

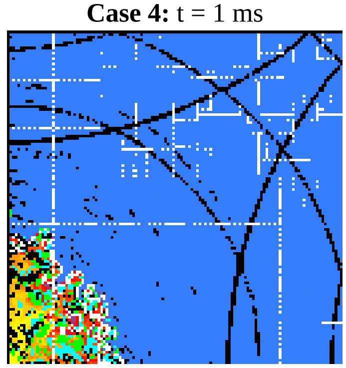

Case 4: t = 4 ms

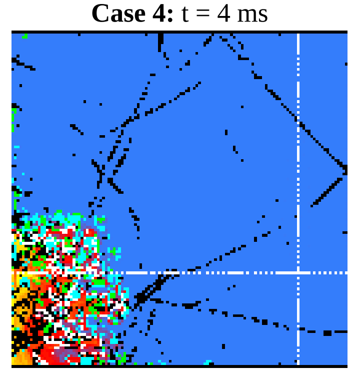

Figure 10. Late-time evolution of the combustion of TNT detonation products corresponding to Fig. 9.

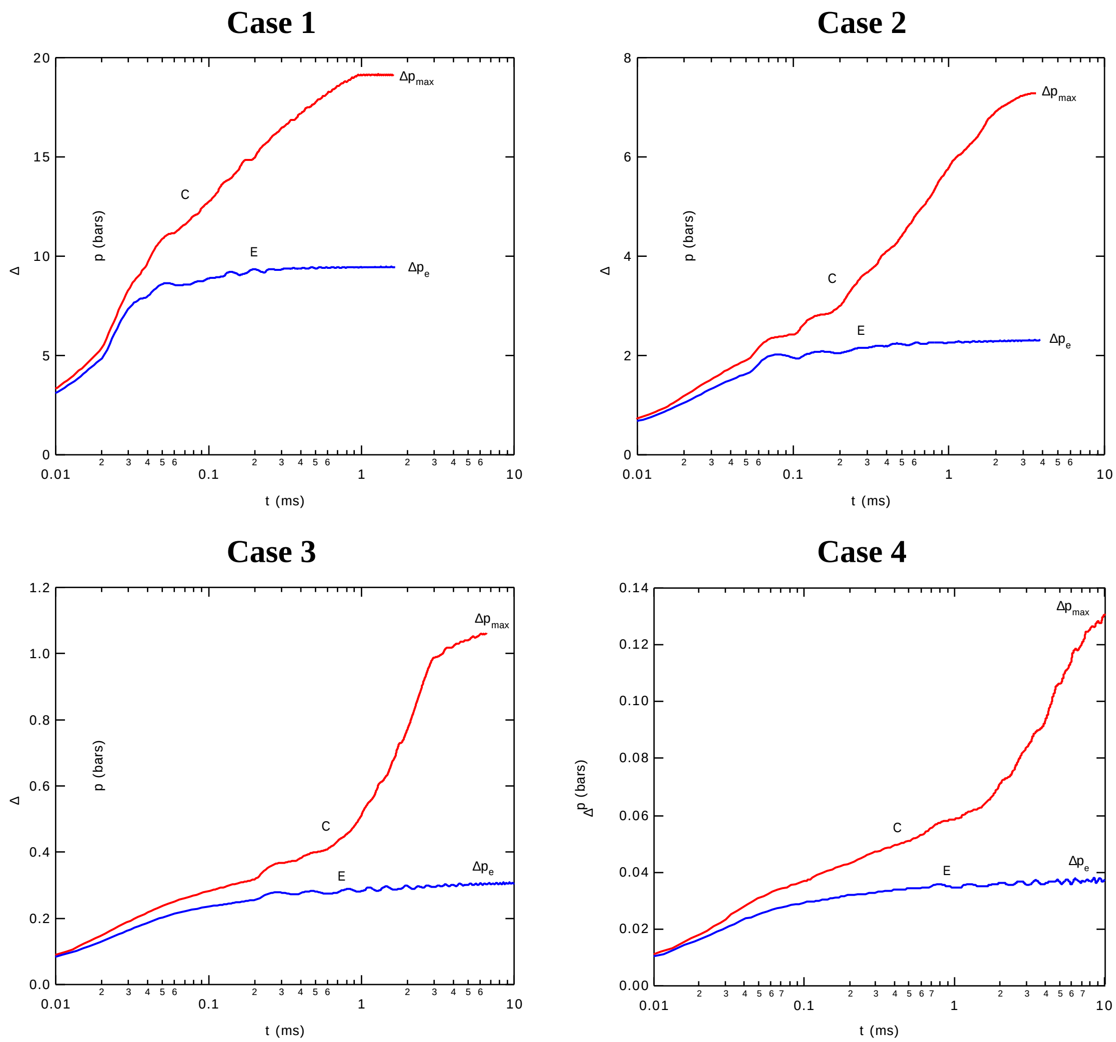

Figure 11. Mean pressure histories for combustion TNT products in various chambers shown in Figs. 9 & 10 (*E* = explosion & *C* = combustion).

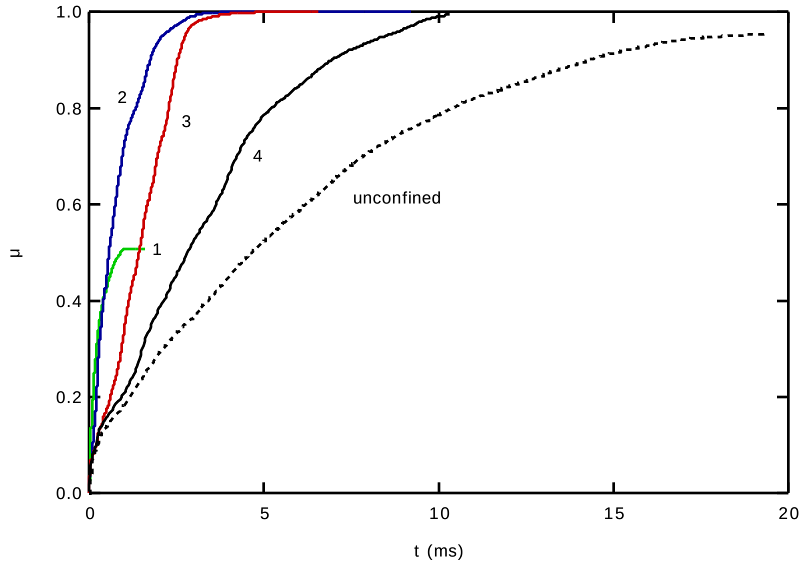

Figure 12. Mass-fraction of fuel consumed by combustion for Cases 1-4.